CALCULATED AND MEASURED ULTRASONIC RESPONSE OF AN ELASTIC

CYLINDER EMBEDDED IN AN ELASTIC MEDIUM

R.C. Addison, Jr.

Rockwell International Science Center
1049 Camino Dos Rios
Thousand Oaks, CA 91360

A.N. Sinclair

Department of Mechanical Engineering
University of Toronto
Toronto, Canada M5S 1A4

INTRODUCTION

Titanium metal matrix composite (TMC) materials are fabricated by consolidating alternate layers of suitable titanium foils and silicon carbide fibers. The foils are generally 0.005-0.010 in thick and the fibers have diameters ranging from 0.004 in. to 0.0055 in. Furthermore, the fibers have a core of one material and an outer annular ring of silicon carbide (Fig. 1). The fibers used in the work described here, designated SCS6 fibers, have an outer diameter of 0.0055 in. and an inner carbon core with a diameter of 0.0013 in. During consolidation, the matrix material is heated under pressure so that it flows around the fibers, forming a strong interfacial bond with the fiber and a strong diffusion bond where the adjacent foils come in contact. Several types of defects can occur during the consolidation process. There can be lack of bonding or incomplete bonding between the adjacent foils or between the matrix and the fibers. It is also possible that an undesirable reaction can occur between the fiber and the matrix, producing a brittle zone that will degrade the strength of the material.

Techniques for the nondestructive inspection of both diffusion-bonded parts and polymer matrix composites have been developed and are widely used. However, the inspection needs of TMC materials differ from these and require new approaches to detect disbonds and weak bonds between adjacent matrix foils and weak interfacial bonds between the reinforcing fibers and the foil. Although ultrasonic C-scans of these defects in TMC materials have a similar appearance to those found in polymer composites, the defects are significantly different both in their origin and in their effect on the properties of the material. The nondestructive inspection and evaluation of TMC materials presents new challenges because of the overall thinness of the panels, the multiple diffusion bonds between plies and the metallurgy of the interfacial bonds between the matrix and the reinforcing fibers.

Review of Progress in Quantitative Nondestructive Evaluation, Vol. 11A
Edited by D.O. Thompson and D.E. Chimenti, Plenum Press, New York, 1992

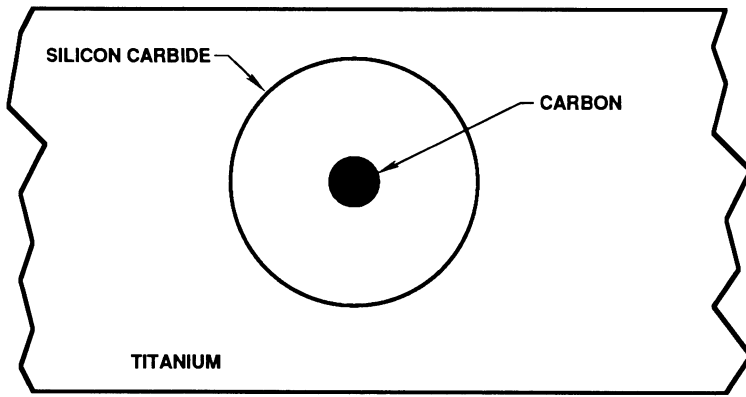105

SILICON CARBIDE

CARBON

TITANIUM

Fig. 1 Diagram of an SCS6 fiber embedded in a titanium matrix.

APPROACH

The thinness of the panels requires the use of high frequency tightly focused ultrasonic transducers that allow us to temporally resolve the individual diffusion bond lines between foils and to spatially resolve the individual fibers. This capability combined with advanced signal processing techniques permits the measurement of the ultrasonic response of the fibers. Measurement of the ultrasonic response of the fiber permits an assessment of the quality of the fiber/matrix interfacial bond and may permit the detection of brittle reaction zones.

CALCULATION OF THE ULTRASONIC RESPONSE

The diffraction spectrum of an infinitely long fiber having a core and outer annular ring (Fig. 1) that is embedded in an elastic medium was calculated by solving the equation of motion for the displacement $\vec{S}$ in the fiber core, fiber outer annulus, and surrounding medium as a function of frequency ω:

$$(\lambda + \mu)\, \nabla\nabla \cdot \vec{S} + \mu\nabla^2\vec{S} = \rho\, \frac{\partial^2\vec{S}}{\partial t^2}$$

(1)

where λ and μ are the lame' constants and ρ the density of the medium. The forcing function is an infinite plane compression wave, arbitrarily assigned an amplitude of unity. Following the solution method first used by Faran [1] and later White [2] and Pao and Mow,[3] the displacement in each medium in cylindrical coordinates (r, θ) is expressed as the sum of the gradient of a scalar field and the curl of a vector field [4]:

$$\vec{S} = \nabla\Phi + \nabla \times \vec{A}$$

(2)

where ϕ and $\vec{A}$ both satisfy the Helmholtz equation, and have solutions

$$\phi = \sum_{n=0}^{\infty} \left[a_n H_n^{(1)}(Kr) + b_n H_n^{(2)}(Kr) \right] \cos n\theta \, e^{-i\omega t}$$

(3a)

and

$$\vec{A} = \sum_{n=0}^{\infty} \left[c_n H_n^{(1)}(Kr) + d_n H_n^{(2)}(Kr) \right] \sin n\theta \; e^{-i\omega t} \vec{z}$$

$$(3b)$$

where K and k are the compression and shear wave numbers, respectively, corresponding to frequency ω and $H_n^{(1)}$ and $H_n^{(2)}$ are Hankel functions of the first and second kind. For each value of n there are twelve unknown parameters: a_n, b_n, c_n, and d_n for each of three media. Using the orthogonality of the sin $n\theta$ and cos $n\theta$ functions, these constants can be solved using the following 12 conditions:

(a)   Eight interfacial boundary conditions, consisting of continuity of radial and tangential stress, continuity of radial and tangential displacement at both the core-annulus and annulus-matrix boundaries.

(b)   In the inner core, $a_n = b_n$ and $c_n = d_n$ to keep the solution finite as $r \rightarrow 0$.

(c)   In the infinite medium, the diffracted wave has only cylindrically diverging components, implying that $b_n = d_n = 0$.

The eight interfacial boundary conditions are written in matrix form and solved as a function of n for a given value of ω. The infinite series of Eq. (3) is truncated for each value of ω once the series has converged, or when numerical problems make calculation of further terms in the series impossible. Expressions for the radial stress originating from the diffracted wave are then determined for arbitrary (r, θ) using Eqs. (2) and (3), plus the strain-displacement relations and linear constitutive equations.

RESPONSE OF FIBERS IMMERSED IN WATER

Verification of the code's accuracy was based on comparison of results with published data [1,5] and experiments. The simplest test case was that of a homogeneous wire immersed in water. For this configuration, we can be sure that the elastic boundary conditions are uniform around the circumference of the wire, thus conforming to the assumptions of cylindrical symmetry made in the model upon which the calculated response is based. Broadband signals were acquired from the wire and deconvolved using a reference waveform. Both the magnitude and phase of the response are obtained, but thus far only the magnitude response is being used. The diffraction spectrum showed a number of sharp dips; the explanation for their origin was formalized by the Resonance Theory of Acoustic Scattering by Flax *et al* [6]: an acoustic resonance occurs when the circumference of the wire is equal to an integral number of wavelengths n of a wave mode traveling around the wire. For a cylinder in water, it is leaky Rayleigh waves which provide the most prominent resonance dips. For a solid cylinder inside a solid matrix, Stonely waves are the mode of interest.

We next measured the response of an SCS6 fiber immersed in water. After deconvolution, the ultrasonic frequency response of the fiber was obtained (Fig. 2, open circles), which displayed resonance dips at about 28, 47, 54, 78, and 96 MHz that are characteristic of the fiber. The calculated response is also shown as a solid line in Fig. 2. The calculated response assumes that the SCS6 fiber has a 140 μm O.D. and contains a 33 μm diameter core of carbon surrounded by a SiC annulus. Since the transverse elastic constants of the carbon core and the SiC were unknown, the value of the shear wave velocity of the carbon and the SiC used in the model were adjusted to produce an acceptable fit between the measured and calculated data. The Rayleigh-like waves that propagate around the circumference of the fiber have an amplitude that decays exponentially towards the center of the fiber with a decay constant that is proportional to the wavelength. Therefore as the frequency increases causing the wavelength to decrease, the depth of penetration of the wave energy into the fiber decreases. Thus the resonances at the higher frequencies are less affected by the carbon core and allow both unknown velocities to be
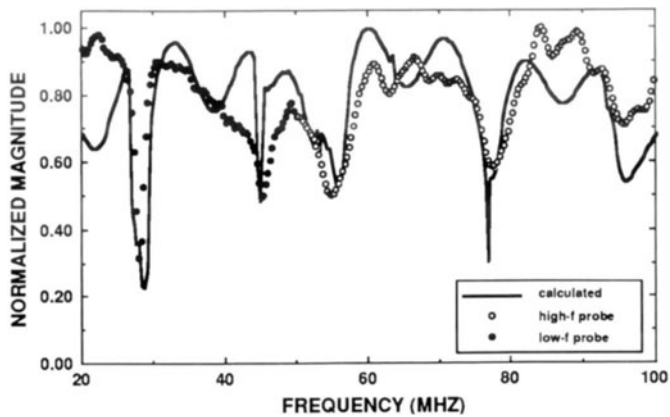
Fig. 2   Measured (open circles) and calculated (solid line) ultrasonic response of an SCS6 fiber immersed in water.

estimated from the same set of data. Due to limitations of an upper bound of 100 MHz for the ultrasonic experiments and the small diameter of the fiber core, no resonances would be visible that are explicitly due to waves traveling around the core-annulus interface. It is still expected, however, that the inner core would affect the phase velocity of the lower modes traveling around the annulus-matrix interface. We found that a shear wave velocity of 7.350 mm/μsec in the SiC and a shear wave velocity of 2.615 mm/μsec in the carbon produced good agreement between the calculated and measured data. These values are within the range of values found in handbooks.

TEST SPECIMENS

        To develop NDE techniques suitable for characterizing the fiber/matrix interface, we required a test specimen that would allow the ultrasonic response of a single fiber to be isolated and studied. A specimen was made of titanium (Ti-6Al-4V) with various types of SiC fibers embedded in it. The specimen was about 1 in x 1 in and about 0.060-0.070 in thick. The fibers were placed between two of the Ti plies. The distance between the fibers and the outer surfaces was sufficient to avoid overlap between the ultrasonic echo from either surface and the ultrasonic echo from the fiber. The specimen was consolidated using conservative procedures that would yield a void free diffusion bond between the abutting plies of Ti. There was no deliberate attempt to achieve any weak bonds, either between the Ti plies or between the Ti and the fibers.

RESPONSE OF FIBERS EMBEDDED IN TITANIUM 6Al-4V

        Our model used for calculating the ultrasonic response of a fiber shows that the size and composition of the fiber affects the amplitude and phase of the ultrasonic waves reflected from them in a predictable way. Further a C-scan image made of the test specimen and subsequent analysis of the ultrasonic response of the fibers suggests that this response is a sensitive indicator of changes in the fiber/matrix boundary condition.

        The measured ultrasonic responses of an uncoated SCS6 fiber shown in Fig. 3 are valid from about 40 MHz to 100 MHz. These responses, in general, display a major resonance dip at about 75-80 MHz (Fig. 3a) that corresponds to the dip predicted in the calculated response. Sometimes there is no dip (Fig. 3b) which is interpreted as a disbonded fiber. In addition to the major resonance dip, there are other subsidiary peaks and dips that are variable from one measurement site to another as well as differences in the slowly varying portion of the curve between 40 and 60 MHz. The significance of these features is not currently known.
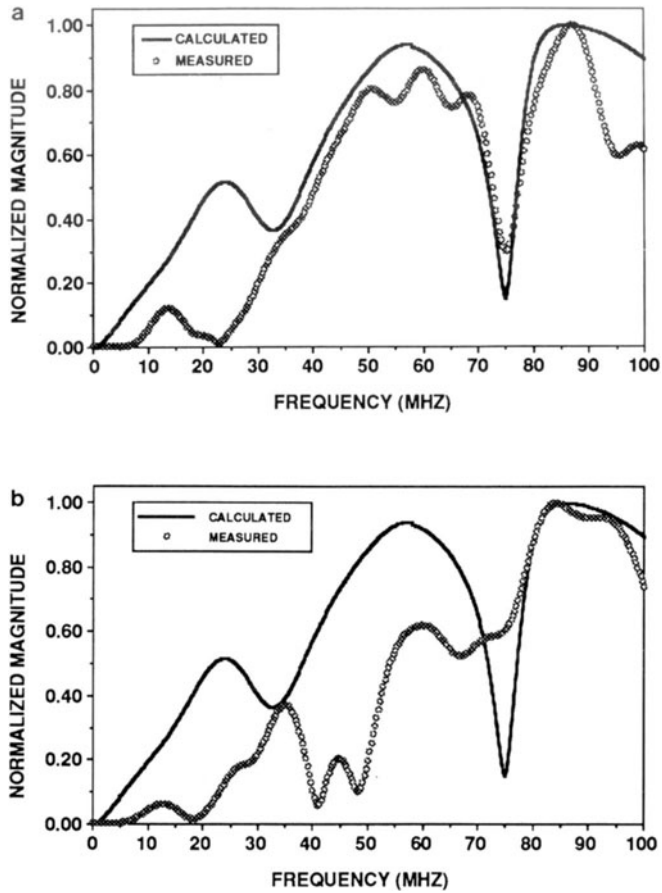
Fig. 3   Measured (open circles) and Calculated (solid line) ultrasonic response at three sites along an uncoated SCS6 fiber. a) Response shows good agreement with resonance dip at 75 MHz and frequencies between 30 MHz and 75 Mhz. b) Response does not display a resonance dip at 75 MHz and deviates from theory

The results of the waveform analysis performed on this specimen as well as other specimens suggest that the characteristics of the fiber/matrix bond are changing continuously along the length of the fiber and from fiber to fiber. To get some global measure of the variability of the response, we prepared a signal processing algorithm that allows the "sharpness" of the resonance dip occurring within a specific frequency band to be mapped spatially and displayed as a C-scan image.

The "sharpness" of the dip is measured using the equation,

$$F = \frac{A_{dip}}{A_1 + A_2} \tag{4}$$

where A_1 and A_2 are the amplitudes of the response a specified frequency interval, Δf, above and below the dip frequency and A_{dip} is the amplitude at the dip. The value of F will range from 0 for a resonant dip that drops to the horizontal axis to 0.5 if no dip is present. The value of F is then mapped into a C-scan format.

A high magnification C-scan image of two SCS6 fibers in the test specimen was made and is displayed as both a conventional amplitude image (Fig. 4a) and a resonance
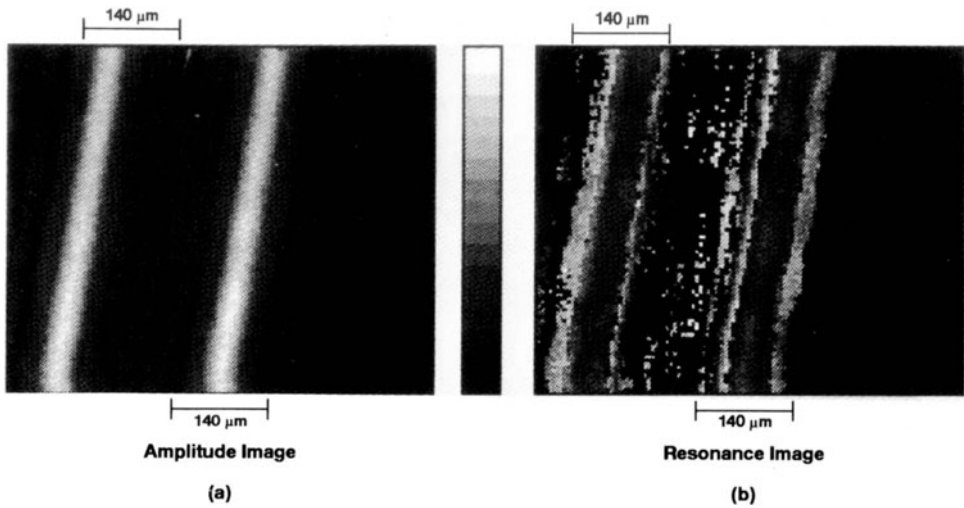
Fig. 4   C-scan images of two SCS6 fibers in the strongly consolidated Ti-6-4 test specimen. a) Conventional amplitude image. b) Resonance image based on the figure-of-merit for bond quality.

image (Fig. 4b). These images show that the response of the fiber, both its echo amplitude and the "sharpness" of its resonance dip are very uniform. In another specimen that was weakly consolidated, the corresponding images show a highly variable response along the fiber.

CONCLUSIONS

We have described a new method for nondestructively characterizing the interfacial bond between fiber and matrix in a titanium matrix composite. This method measures the ultrasonic response of an elastic fiber in an elastic matrix. This response can be very sensitive to small changes in the fiber/matrix bond. To display the data in a useful way, a method was developed for extracting a figure-of-merit for the bond quality from the ultrasonic response of the fiber. This figure-of-merit can be displayed as a C-scan image. The method was demonstrated with a strongly consolidated single-ply Ti-6-4/SCS6 specimen. The results are encouraging.

Further work is needed to completely understand the underlying causes of the variation of the ultrasonic response and how it relates to changes in the fiber/matrix bond. The modes observed in the ultrasonic response need to be identified so the changes in those that are most sensitive to the fiber/matrix interface can be measured. Further the effect of non-ideal bonds on the ultrasonic response needs to be determined. In particular the effects of a compliant interface or a brittle reaction zone should be calculated and compared with measured responses.

Currently the results of this work are chiefly applicable to evaluate the adequacy of a particular set of process conditions with a single-ply specimen. Future work can extend the technique so that it can be used to nondestructively evaluate multi-ply specimens.

REFERENCES

1.   J.J. Faran, Jr., "Sound Scattering by Solid Cylinders And Spheres," JASA, 23, 405-417 (1951).

2.   R.M. White, "Elastic Wave Scattering At A Cylindrical Discontinuity In A Solid," JASA 30, 771-785 (1958).

3.   Y.H. Pao and C.C. Mow, in <u>Diffraction Of Elastic Waves And Dynamic Stress Concentrations,</u> Crane, Russack & Co., New York, 1973. Sections III-1 to III-4.

4.   P.M. Morse and H. Feshbach, in <u>Methods Of Theoretical Physics,</u> McGraw Hill, New York, 1953. Chapter 13.

5.   V.V. Varadan, "Scattering Matrix For Elastic Waves, II; Application To Elliptic Cylinders," JASA <u>63</u>, 1014-1024 (1978).

6.   L. Flax, G.C. Gaunaurd, and H. Uberall, "Theory Of Resonance Scattering," in <u>Physical Acoustics,</u> ed. W.P. Mason and R.N. Thurston, vol. XV, pp. 191-295, Academic Press, New York, 1981.